



Cite this: *Phys. Chem. Chem. Phys.*,
2018, 20, 28979

Received 15th September 2018,
Accepted 8th November 2018

DOI: 10.1039/c8cp05837g

rsc.li/pccp

Antiferromagnetic ordering based on intermolecular London dispersion interactions in amphiphilic TEMPO ammonium salts†

Jessica Exner,^a Steffen Eusterwiemann,^a Oliver Janka,^{ib} Carsten Doerenkamp,^{cd}
Anja Massolle,^{ae} Oliver Niehaus,^b Constantin G. Daniliuc,^{ib} Rainer Pöttgen,^{ib} *^b
Johannes Neugebauer,^{ib} *^{ae} Armido Studer^{ib} *^a and Hellmut Eckert^{ib} *^{cd}

Antiferromagnetic coupling in TEMPO-based radicals can be enhanced via self-assembly through London dispersion interactions in amphiphilic solids. The synthesis, magnetic characterization, and three crystal structures of the solid radical ion salts (R-DMAT-*n*)X with various counterions X and alkyl chain lengths *n* are reported. Magnetic susceptibility and absolute EPR signal intensity measurements show singlet–triplet transitions in a number of cases, which is discussed in relation to the crystal structures. Antiferromagnetic ordering effects are sensitive to both the length of the alkyl chain and the counter anion.

Organic radicals are attracting much attention in the field of materials science since they have found applications as spin labels, spin traps, and electronic, optical or magnetic materials.¹ Spin building blocks like nitroxide radicals,^{2–5} verdazyl radicals^{6,7} or sulfur/nitrogen containing radicals^{8–10} are stable enough to be stored under ambient conditions and have been studied intensively because of their interesting magnetic properties.^{11,12} Cooperative magnetic effects, *i.e.* antiferromagnetism or ferromagnetism in fully organic materials depend on the interaction between the unpaired electrons in the solid state and are therefore difficult to control.¹³ An understanding of the relationship between the packing of molecules in the crystal structure and the

resulting magnetic properties is consequently of fundamental interest. This process is often accomplished by quantum chemical calculations, which help to identify the magnetic topologies.^{14,15} In recent studies, the magnetic properties could be tuned by the use of hydrogen bond interactions,¹⁶ π – π stacking interactions,¹⁷ fluorine–fluorine repulsion or ligation to transition metals.¹⁸ Carbon centred radicals such as polychlorinated triphenylmethyl radicals and nitrogen/oxygen centred radicals, especially nitronyl and imino nitroxides, have been studied most commonly since they do not show any disproportionation or hydrogen abstraction reactions.¹¹ In contrast, in simple aminoxyl radicals such as 2,2,6,6-tetramethylpiperidinyloxy (TEMPO), the presence of bulky alkyl groups in the α -position tends to attenuate such intermolecular magnetic interactions, owing to steric hindrance. Thus, only a few examples of magnetic ordering effects in such solids have been documented to date.^{19–23} It is well known, however, that nitroxide radicals bearing long alkyl chains can self-assemble into micellar structures.^{24,25} With the ability to organize the structure of organic compounds by London dispersion,²⁶ the question arises whether the latter interactions are also strong enough to affect the magnetic properties in a suitable system. First results are reported herein.

As a model compound class an amphiphilic system was designed, where the TEMPO radical is attached to a 4-dimethyl amino group bound to a linear alkyl chain with *n* C-atoms, forming a radical ammonium salt R-DMAT-*n* iodide ($R = C_nH_{2n+1}$; DMAT = dimethyl-amino-TEMPO). Such compounds have been studied before as spin probes and in fluorescence quenching studies.^{23,25} However, no investigations of their magnetic properties are known, except for R-DMAT-1, which shows antiferromagnetic ordering at low temperature ($T_N \sim 12$ K).¹⁹ Here we present the first systematic magnetic study of these radical cation salts. It suggests that (1) the intermolecular dispersion interactions in these compounds are apparently strong enough to facilitate cooperative magnetic behaviour, and (2) the observation of antiferromagnetic coupling requires alkyl chains of a certain length. The magnetic behaviour can be modified further by changing the counter anion.

^a Organic Chemistry Institute, Westfälische Wilhelms-University Münster, Corrensstrasse 40, 48149 Münster, Germany. E-mail: studer@uni-muenster.de, j.neugebauer@uni-muenster.de

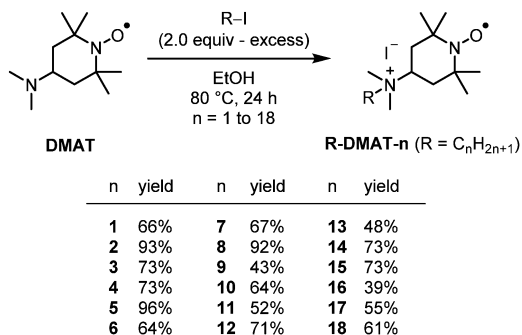
^b Institut für Anorganische und Analytische Chemie, Westfälische Wilhelms-Universität Münster, Corrensstrasse 30, 48149 Münster, Germany. E-mail: pottgen@uni-muenster.de

^c Institute of Physical Chemistry, Westfälische Wilhelms-University Münster, Corrensstrasse 28/30, 48149 Münster, Germany. E-mail: eckerth@uni-muenster.de

^d São Carlos Institute of Physics, University of São Paulo, Av. Trab. São-Carlense 400, 13566-590 São Carlos, SP, Brazil. E-mail: eckerth@uni-muenster.de

^e Center for Multiscale Theory and Computation, Corrensstrasse 40, 48149 Münster, Germany

† Electronic supplementary information (ESI) available: Details on syntheses and characterizations, crystal structures, EPR data, magnetic characterization, quantum chemical calculations. CCDC 1826204–1826207. For ESI and crystallographic data in CIF or other electronic format see DOI: 10.1039/c8cp05837g



Scheme 1 Preparation of the amphiphilic TEMPO ammonium salts R-DMAT-*n*.

We commenced the studies by preparing a series of TEMPO ammonium salts with different *N*-alkyl chain lengths (*n* = 1–18), through stirring of DMAT with a slight excess of the corresponding alkyl iodide in EtOH. They were obtained as orange solids or oils (Scheme 1, for Experimental details, see ESI†). The samples were purified by medium pressure liquid chromatography (MPLC) using a stationary phase functionalized with amino groups.

Fig. 1 shows the temperature-dependent magnetic susceptibilities of some members of this R-DMAT-*n* series. Clear maxima are found at low temperature, characteristic of the typical singlet–triplet transitions observed for antiferromagnetic coupling. For example, in the case of R-DMAT-16 iodide, a Néel temperature of $T_N = 8.6(1)$ K is found. As illustrated by Fig. 1, the Bleaney–Bowers model for spin-1/2 particles that are antiferromagnetically coupled into intermolecular dimers provides an approximate description for these curves.²⁷

$$\chi = \frac{4C}{T \left(3 + \exp\left(-\frac{2J}{k_B T}\right) \right)}$$

C is the Curie constant and *J* the exchange coupling constant. These are the two independent fitting parameters, which are

Table 1 Experimental Néel temperatures T_N , antiferromagnetic coupling constants *J* (in cm^{-1}) and Curie constants *C* (in K emu mol^{-1}), extracted from fits of temperature dependent magnetic susceptibility data to the Bleaney–Bowers dimer model in solid R-DMAT-*n* iodide salts

Sample	T_N/K	J/cm^{-1}	<i>C</i>
R-DMAT-1	12.5	−7.0	0.294
R-DMAT-10	4.1	−2.6	0.260
R-DMAT-12	4.7	−2.7	0.272
R-DMAT-13	5.2	−2.7	0.257
R-DMAT-14	6.7	−3.8	0.323
R-DMAT-15	5.8	−3.2	0.312
R-DMAT-16	8.6	−4.8	0.351
R-DMAT-17	4.7	−2.7	0.252

summarized in Table 1. In most cases, the agreement is only approximate, indicating a Curie constant smaller than the theoretical value of $0.375 \text{ K emu mol}^{-1}$ expected for a spin-1/2 radical species. The deviations may be attributable to the presence of diamagnetic impurities or partial decomposition of the radicals. For molecules with shorter aliphatic chains, such as R-DMAT-*n* (*n* < 10) the temperature dependent susceptibility data still follows the typical Curie-paramagnetic behaviour of radical compounds (see ESI†). Similar trends are observed for the magnetization isotherms (see Fig. S18, ESI†).

Aside from R-DMAT-1, intermolecular antiferromagnetic coupling is only observed at a chain length $n \geq 10$, with a maximum near $n = 16$, where a *J* value of -4.8 cm^{-1} is found. Interestingly $n = 17$ also corresponds to the longest non-folded alkane chain.²⁸ All of these findings suggest that London dispersion interactions involving the linear *N*-alkyl chains are key to get magnetic coupling in the corresponding salts. While no crystal structure was available for this particular material, we were able to solve and refine the crystal structures of R-DMAT-15 iodide (see Fig. 2) as well as those of the mixed-anion compounds (R-DMAT-15)_{0.45}(CF₃SO₃)_{0.55} and (R-DMAT-14)_{0.5}(CF₃SO₃)_{0.5}. Fig. 2 and 3 show details of the crystal structure of R-DMAT-15 iodide measured at 100 K. The asymmetric unit contains two molecules A and B, whose packing diagram reveals two principal structural motifs. One motif involves an antiparallel orientation of two neighbouring nitroxide radicals forming a S-like shape (Fig. 3, top), with an intermolecular O1B···O1B distance of 4.394 Å. The second motif shows a U-like shape with a distance of 5.832 Å between the spin-bearing atoms O1A···O1A. Not surprisingly, the latter distance is too long for any relevant magnetic interaction. The same features and very similar shortest O···O distances occur in (R-DMAT-15)_{0.45}(CF₃SO₃)_{0.55} (4.298 Å) and (R-DMAT-14)_{0.5}(CF₃SO₃)_{0.5} (4.328 Å) (see ESI†). In contrast, these distances are absent in the crystal structure of R-DMAT-16 chloride dihydrate, which behaves like a Curie paramagnet. In experimentally determined structures, the alkyl chains are present in the expected zig-zag conformation and the dispersion interactions are obvious from the arrangement of the linear alkyl chains in the crystal (Fig. 3, bottom). Evidently these distances are sufficient for facilitating weak antiferromagnetic coupling interactions. An estimate of the London dispersion interactions

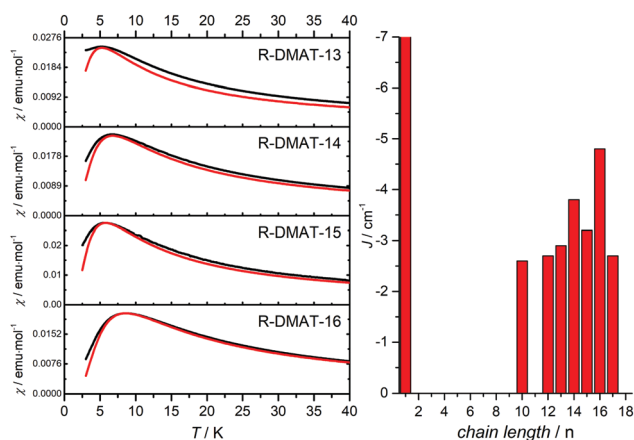


Fig. 1 Left: Temperature dependent molar susceptibilities for various R-DMAT-*n* iodide salts, displaying antiferromagnetic ordering. Red curves are fits to the Bleaney–Bowers dimer model. Right: Plot of *J* against the chain length *n*.

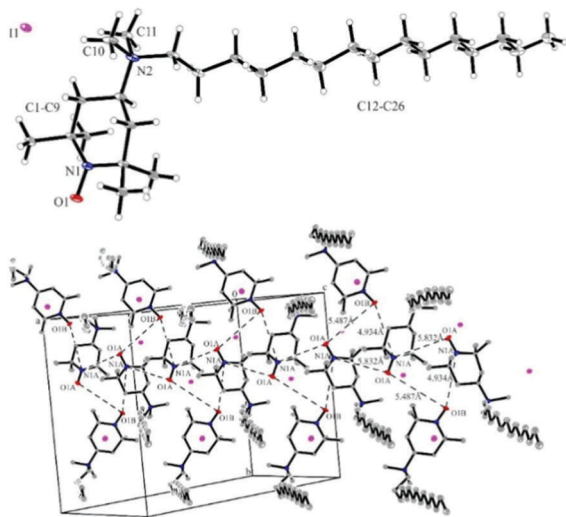


Fig. 2 Molecular structure (A molecules, top) and packing diagram (bottom) representing the O...O and N...O interactions along the *c*-axis in R-DMAT-15-I (O1A...O1B 5.487 Å; O1A...N1A 5.832 Å; O1B...N1A 4.934 Å).

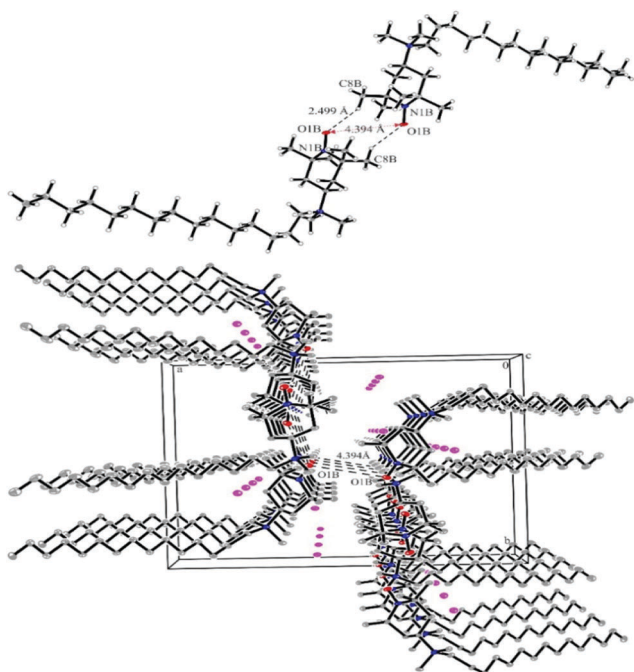


Fig. 3 Molecular S-like arrangement (top) and packing diagram (bottom) of the crystal structure of R-DMAT-15 iodide, representing the O...O interactions between the molecules "B" along the *a*-axis in R-DMAT-15-I (O1B...O1B 4.394 Å).

between the monomers for the crystallographically characterized compounds is given in Table S7 in the ESI[†] (Section 6.2) and confirms the expected increase in strength with increasing length of the alkyl chain.

The spin topology of R-DMAT-15 was determined by quantum chemical calculations using the "black-box" approach described in ref. 15. It shows a zigzag chain with antiferromagnetic couplings ($J_2 = -0.98 \text{ cm}^{-1}$) along the *yz* direction (see Fig. 4).

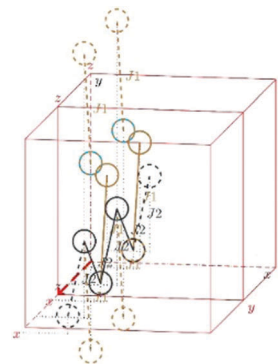


Fig. 4 The spin topology of R-DMAT-15. Only J_1 and J_2 have been included in this model. Of the two identical chains only one is shown. Each circle represents the center of mass of a molecule. Dashed lines represent magnetic interactions to molecules outside the unit cell. The magnetic cell vectors are shown in red, while the crystallographic cell vectors are shown in black.

The chain has an additional antiferromagnetic coupling ($J_1 = -1.54 \text{ cm}^{-1}$) in *y* direction of the crystallographic unit cell. Additionally, a second chain can be obtained by a *C*₂ rotation around the centre of the unit cell. The two chains in the unit cell are connected by weak antiferromagnetic interactions, for further information see Section 6.1 in the ESI[†].

The predicted temperature dependent molar magnetic susceptibility curve is depicted in Fig. 5. As the convergence check is difficult, we only considered the strongest couplings J_1 and J_2 for the magnetic model, for which it is sufficient to model two unit cells along the *x* direction. For this model we observe a transition temperature to the paramagnetic state of about 2.5 K in good qualitative agreement with the experimental data.

To investigate the effect of the counter anion on the transition temperature, we performed anion exchange reactions of R-DMAT-16 iodide with various silver salts (see ESI[†]). In none of the mixed salts with Cl^- , Br^- , BF_4^- , SbF_6^- , PF_6^- cooperative effects were observable (see Fig. S22–S27, ESI[†]). We further studied mixed-anion systems with different triflate-to-iodide ratios. Fig. 6 shows that the strength of the

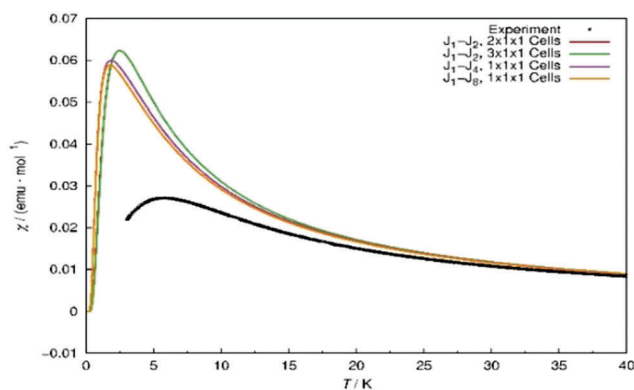


Fig. 5 Predicted and measured temperature (*T*) dependent molar magnetic susceptibility $\chi(T)$ for R-DMAT-15 iodide salt.

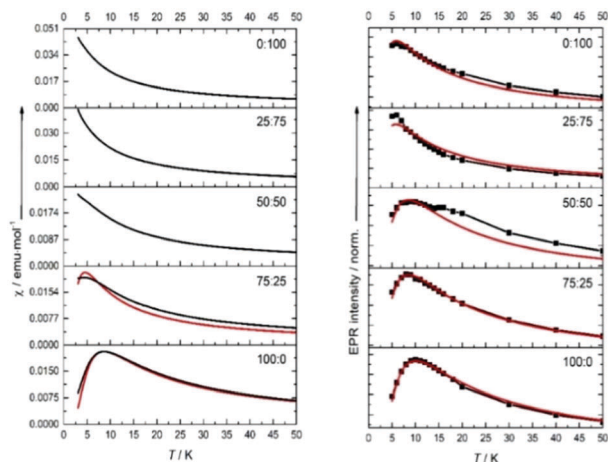


Fig. 6 (a) Temperature dependent magnetic susceptibility of R-DMAT-16 iodide/triflate solid solutions as measured by magnetic susceptibility data (left) and (b) by absolute EPR signal quantification (right). The EPR intensities were normalized to the maximum value. Solid red curves show fits to the Bleaney–Bowers model.²⁶

Table 2 Experimental Néel temperatures T_N , Curie constants C (in K emu mol^{-1}) and antiferromagnetic coupling constants J (in cm^{-1}), extracted from fits of temperature dependent magnetic susceptibility data to the Bleaney–Bowers dimer model in solid mixed R-DMAT-16 iodide/triflate salts. Entries 1 and 2: data from magnetic susceptibility measurements. Entries 3–7: data from EPR signal intensity measurements

Entry	Sample	T_N/K	J/cm^{-1}	C
1	R-DMAT-16 75 : 25	4.5	−2.5	0.190
2	R-DMAT-16 100 : 0	8.6	−4.8	0.351
3	R-DMAT-16 0 : 100	5.8	−3.3	
4	R-DMAT-16 25 : 75	5.8	−3.3	
5	R-DMAT-16 50 : 50	8.5	−4.7	
6	R-DMAT-16 75 : 25	8.5	−4.7	
7	R-DMAT-16 100 : 0	10.0	−5.6	

intermolecular antiferromagnetic coupling as measured either by magnetic force detection or absolute EPR signal quantification is sensitively affected by the anionic composition (Table 2).

We note that the clear susceptibility maximum evident in the pure iodide salt becomes increasingly obscured with increasing triflate content, with a corresponding decrease of $|J|$ from 5.6 cm^{-1} (for the pure iodide) to 3.3 cm^{-1} for the pure triflate salt. Fig. 6 shows that the susceptibility maximum is more easily detected *via* EPR spectra as the latter seem to be less affected by impurities and defect sites.

In recording these EPR data, the microwave power was varied systematically to ensure that maxima observed in the EPR signal intensities were not caused by any saturation effects at these low temperatures (see Fig. S4, ESI[†]). Although for the $n = 15$ series, the X-ray data reveal slightly shorter O1B...O1B distances in case of the mixed triflate/iodide salts (see above), magnetic couplings are weaker in the hetero salts. The reason for this behaviour is currently not understood.

The results of the present study illustrate that intermolecular antiferromagnetic couplings of TEMPO-based radical ions can be realized through self-assembly *via* London dispersion

interactions in amphiphilic systems containing linear alkyl chain substituents. The strength of these interactions can be controlled by the length of the alkyl chain and the counter anion composition. Based on these initial results we are currently developing similar architectures with different spin building blocks in our laboratory.

Conflicts of interest

The authors declare no conflict of interest.

Acknowledgements

We thank the Deutsche Forschungsgemeinschaft (DFG) within the SFB 858 (project B11) for supporting our research. C. D. also acknowledges support by FAPESP (2017/06649-0).

Notes and references

- I. Ratera and J. Veciana, *Chem. Soc. Rev.*, 2012, **41**, 303–349.
- R. Chiarelli, M. A. Novak, A. Rassat and J. L. Tholence, *Nature*, 1993, **363**, 147–149.
- M. Tamura, Y. Nakazawa, D. Shiomi, K. Nozawa, Y. Hosokoshi, M. Ishikawa, M. Takahashi and M. Kinoshita, *Chem. Phys. Lett.*, 1991, **186**, 401–404.
- D. Luneau and P. Rey, *Coord. Chem. Rev.*, 2005, **249**, 2591–2611.
- M. Deumal, J. Cirujeda, J. Veciana and J. J. Novoa, *Chem. – Eur. J.*, 1999, **5**, 1631–1642.
- B. D. Koivisto and R. G. Hicks, *Coord. Chem. Rev.*, 2005, **249**, 2612–2630.
- D. Matuschek, S. Eusterwiemann, L. Stegemann, C. Doerenkamp, B. Wibbeling, C. G. Daniliuc, N. L. Doltsinis, C. A. Strassert, H. Eckert and A. Studer, *Chem. Sci.*, 2015, **6**, 4712–4716.
- A. Banister, N. Bricklebank, I. Lavender, J. M. Rawson, C. I. Gregory, B. K. Tanner, W. Clegg, M. R. J. Elsegood and F. Palacio, *Angew. Chem., Int. Ed. Engl.*, 1996, **35**, 2533–2535.
- W. Fujita and K. Awaga, *Science*, 1999, **286**, 261–262.
- A. Alberola, R. J. Less, C. M. Pask, J. M. Rawson, F. Palacio, P. Oliete, C. Paulsen, A. Yamaguchi, R. D. Farley and D. M. Murphy, *Angew. Chem., Int. Ed.*, 2003, **42**, 4782–4785.
- R. G. Hicks, in *Stable Radicals*, John Wiley & Sons, Ltd, Chichester, UK, 2010.
- R. G. Hicks, *Org. Biomol. Chem.*, 2007, **5**, 1321–1338.
- O. Kahn, *Molecular Magnetism*, VCH Publishers, Inc., New York City, USA, 1993.
- J. J. Novoa, M. Deumal and J. Jornet-Somoza, *Chem. Soc. Rev.*, 2011, **40**, 3182.
- T. Dresselhaus, S. Eusterwiemann, D. R. Matuschek, C. G. Daniliuc, O. Janka, R. Pöttgen, A. Studer and J. Neugebauer, *Phys. Chem. Chem. Phys.*, 2016, **18**, 28262–28273.
- D. M. Gil, H. Osiry, F. Pomiro, E. L. Varetti, R. E. Carbonio, R. R. Alejandro, A. Ben Altabef and E. Reguera, *J. Solid State Chem.*, 2016, **239**, 159–164.

- 17 J. L. Brusso, O. P. Clements, R. C. Haddon, M. E. Itkis, A. A. Leitch, R. T. Oakley, R. W. Reed and J. F. Richardson, *J. Am. Chem. Soc.*, 2004, **126**, 8256–8265.
- 18 B. D. Koivisto, A. S. Ichimura, R. McDonald, M. T. Lemaire, L. K. Thompson and R. G. Hicks, *J. Am. Chem. Soc.*, 2006, **128**, 690–691.
- 19 S. Aonuma, H. Casellas, C. Faulmann, B. Garreau de Bonneval, I. Malfant, P. Cassoux, P. G. Lacroix, Y. Hosokoshi and K. Inoue, *J. Mater. Chem.*, 2001, **11**, 337–345.
- 20 S. Nakatsuji, T. Amano, H. Akutsu and J. Yamada, *J. Phys. Org. Chem.*, 2006, **19**, 333–340.
- 21 S. Nakatsuji, M. Mizumoto, H. Ikemoto, H. Akutsu and J. Yamada, *Eur. J. Org. Chem.*, 2002, 1912–1918.
- 22 M. Nobusawa, H. Akutsu, J. Yamada and S. Nakatsuji, *Lett. Org. Chem.*, 2006, **3**, 685–688.
- 23 A. M. Wasserman, M. V. Motyakin, I. I. Barashkova, L. A. Wasserman and L. L. Yasina, *Russ. Chem. Bull.*, 2015, **64**, 2284–2293.
- 24 W. De Vries, C. Doerenkamp, Z. Zeng, M. de Oliveira Jr, O. Niehaus, R. Pöttgen, A. Studer and H. Eckert, *J. Solid State Chem.*, 2016, **237**, 93–98.
- 25 M. F. Ottaviani, N. J. Turro, S. Jockusch and D. A. Tomalia, *J. Phys. Chem.*, 1996, **100**, 13675–13686.
- 26 J. P. Wagner and P. R. Schreiner, *Angew. Chem., Int. Ed.*, 2015, **54**, 12274–12296.
- 27 B. Bleaney and K. D. Bowers, *Proc. R. Soc. London, Ser. A*, 1952, **214**, 451–465.
- 28 N. O. B. Lüttschwager, T. N. Wassermann, R. A. Mata and M. A. Suhm, *Angew. Chem., Int. Ed.*, 2013, **52**, 463–466.